J Bioenerg Biomembr (2011) 43:163–173
DOI 10.1007/s10863-011-9343-x

Revised assignment of room-temperature chlorophyll fluorescence emission bands in single living cells of *Chlamydomonas reinhardtii*

Lorenzo Ferroni · Costanza Baldisserotto · Martina Giovanardi · Laura Pantaleoni · Tomas Morosinotto · Simonetta Pancaldi

Received: 29 October 2010 / Accepted: 8 January 2011 / Published online: 19 February 2011

Abstract Room temperature (RT) microspectrofluorimetry in vivo of single cells has a great potential in photosynthesis studies. In order to get new information on RT chlorophyll fluorescence bands, we analyzed the spectra of *Chlamydomonas reinhardtii* mutants lacking fundamental proteins of the thylakoid membrane and spectra of photoinhibited WT cells. RT spectra of single living cells were characterized thorough derivative analyses and Gaussian deconvolution. The results obtained suggest that the dynamism in LHCII assembly could be sufficient to explain the variations in amplitudes of F680 (free LHCII), F694 (LHCII-PSII) and F702 (LHCII aggregates); F686 was assigned to the PSII core. Based on the revised assignments and on the variations observed, we discuss the meaning of the two fluorescence emission ratios F680/(F686+F694) and F702/(F686+F694), showing that these are sensitive parameters under moderate photoinhibition. In the most photoinhibited samples, the RT spectra tended to degenerate, showing characteristics of mutants that are partly depleted in PSII.

L. Ferroni · C. Baldisserotto · M. Giovanardi · S. Pancaldi (✉)
Laboratory of Plant Cytophysiology, Department of Biology and Evolution, University of Ferrara,
C.so Ercole I d'Este, 32,
44121 Ferrara, Italy
e-mail: pcs@unife.it

L. Pantaleoni
Department of Genetics and Microbiology, University of Pavia,
Via Ferrata 1,
27100 Pavia, Italy

T. Morosinotto
Department of Biology, University of Padova,
Via Ugo Bassi 58/B,
35121 Padova, Italy

Keywords *Chlamydomonas reinhardtii* · Fluorescence · Light-harvesting complex II · Room-temperature microspectrofluorimetry · Photoinhibition · Photosystem II · Thylakoid membrane

Introduction

Photosynthetic membranes of all organisms capable of oxygenic photosynthesis host two photosystems (PSI and PSII) working in series to drive electrons from water to $NADP^+$. PSII is the large multisubunit pigment-protein complex which catalyzes the light-induced electron transfer form water to plastoquinone. The photochemical PSII reaction centre (RC) is composed of two similar proteins, D1 and D2, and of the cytochrome b_{559}. The D1/D2 heterodimer coordinates the manganese cluster of the oxygen evolving center (OEC) at the luminal side of the membrane and contains all the electron transfer components needed for the charge separation (Barber 2002). Two intrinsic, sequence-related chlorophyll *a*-binding antenna proteins, CP43 and CP47, are closely associated with RC (Bricker and Frankel 2002). In organisms belonging to Viridiplantae most of the chlorophylls that are associated with PSII are assembled in the peripheral light harvesting complex II (LHCII), a chlorophyll *a*/*b*-containing antenna system. LHCII is organized in trimers of the light-harvesting proteins Lhcb1, Lhcb2 and Lhcb3, which are similar in structure and represented in different stoichiometry in the trimers. LHCII is involved not only in enhancing light-harvesting, but also in avoiding the over-accumulation of excitation energy in PSII (Schmid 2008). Minor light-harvesting subunits (CP24, CP26 and CP29) mediate the energy transfer from LHCII to the PSII core and also

participate in excess energy dissipation (Andersson et al. 2001; de Bianchi et al. 2008). The core of PSI consists mainly of the PsaA-PsaB heterodimer, hosting the photochemical center and most of the PSI pigments; LHCI is the extrinsic peripheral light-harvesting complex of PSI and is composed of modular arrangements of the Lhca1-4 chlorophyll proteins (Ben-Shem et al. 2003).

Low temperature (77 K) fluorescence emission spectra are widely used to investigate the association of chlorophyll-protein complexes in vivo. The spectra recorded at 77 K show a prominent band with a maximum at 710–740 nm, which is emitted by PSI and its antenna LHCI, with a wavelength depending on the species. PSII originates two characteristic emissions at 685 nm (F685) and 695 nm (F695), which are more or less resolved as independent peaks in different plant samples and have generally been attributed to CP43 and CP47, respectively (Alfonso et al. 1994; Groot et al. 1999; van Dorssen et al. 1987). More recently, it has been shown that F685 could originate from excitations that are slowly transferred from 683 nm states in both CP43 and CP47 to RC (Andrizhiyevskaya et al. 2005). In addition to the two PSII core peaks, 77 K spectra can also show a shoulder at ca. 680 nm, which is assigned to "free" LHCII, i.e. not stably associated with the PSII core (Hemelrjik et al. 1992). The amplitude of this emission is indeed linked to the release of LHCII from LHCII-PSII complexes (Šiffel and Braunová 1999; van der Weij-de Wit et al. 2007) and also correlates with high amounts of free LHCII trimers at the steady state in the thylakoid membranes (Pantaleoni et al. 2009).

It is well-known that the rise from 77 K to room temperature (RT, i.e. ca. 295 K) causes a drastic change in the shape of the fluorescence emission spectra (Boardman et al. 1966). The increase in temperature from 77 K to RT results in the gradual disappearance of the F695 peak, leading to the only maximum at 684 nm (Andrizhiyevskaya et al. 2005). The RT spectra indeed show only one peak at approximately 684 nm, attributed mainly to PSII, and a very broad shoulder at 710–740 nm. Different from 77 K, at RT many chlorophylls belonging to different complexes are expected to provide overlapping contributions to the emission profiles. PSII fluorescence persisting at physiological temperatures around 685 nm has been proposed to arise from both CP43 pigments and excited states of RC, both clustering near 685 nm (Krausz et al. 2005).The 710–740 nm region is presently considered to be a combination of PSI-LHCI emissions and vibrational satellites of PSII (Franck et al. 2005; Ferroni et al. 2009). LHCII does not originate an individual peak at RT.

RT emission spectra have only seldom found application in photosynthesis research (Franck et al. 2005; Ferroni et al. 2009; Lambrev et al. 2010). In spite of the overlapping emission sources, one possibility for exploiting RT spectra can be the analytical study of the curves, in order to resolve individual components. In our laboratories, a procedure based on derivative analyses and deconvolution of components has been used to characterize the RT spectra recorded from microscopic samples using a spectrofluorimeter associated with a fluorescence microscope (Pancaldi et al. 2002). In most cases, the spectral region of PSII (675–695 nm) was resolved into three main components at approximately 679, 685 and 695 nm (Pancaldi et al. 2002; Baldisserotto et al. 2004; Ferroni et al. 2007a, 2009). Other minor components were also resolved, such as emissions at 670 and 700 nm. Microspectrofluorimetry has a great potential in photosynthesis studies. In fact spectra can be recorded from even single cells and this offers the valuable possibility of collecting data separately from heterogeneous cell populations, for instance belonging to different tissues in the framework of a higher plant leaf (Baldisserotto et al. 2004; Pantaleoni et al. 2009). The application of microspectrofluorimetric methods could take a great advantage from an improved attribution of RT bands to specific complexes.

In order to get new information on the origin of RT fluorescence emission bands, especially in the region attributed to PSII (675–695 nm), in this work we have analyzed the RT spectra recorded from wild-type (WT) *Chlamydomonas reinhardtii* and mutants of this unicellular alga. This is a well-known model organism for photosynthesis studies, also due to the availability of characterized photosynthetic mutants. The mutants we have studied lack fundamental thylakoid proteins but are still able to grow in heterotrophy and thus offer the possibility of analyzing how much different polypeptide deficiencies alter the RT spectra with respect to a WT strain. A similar approach has been profitably used in the past for the biochemical characterization of PSII assembly (de Vitry et al. 1989) and for the 77 K spectrofluorimetric characterization of PSI antenna complexes (Garnier et al. 1986). Furthermore, *Chlamydomonas* strains respond to the requisite of homogeneity of cells in culture and thus represent a suitable experimental material for approaching the problem of fluorescence bands assignment.

Materials and methods

Strains and culture conditions The *Chlamydomonas reinhardtii* strains used in this study were obtained from the *Chlamydomonas* Genetics Center (Duke University, Durham, NC): (a) cc-1690, WT strain; (b) cc-2519, D2-deficient *FUD47* strain; (c) cc-3033, CP43-deficient *F34* strain; (d) cc-1354, chlorophyll *b*-less *cbn1-48* strain; (e) cc-4151, PSI-deficient *FUD26* strain. Cultures were maintained in solid Tris acetate/phosphate medium (TAP) at low

irradiance (5 μmol photons m^{-2} s^{-1}) at 24 °C. Liquid cultures for physiological studies were prepared in the same TAP medium in 100-mL Erlenmeyer flasks shaken at 90 rpm under low light (20 μmol photons m^{-2} s^{-1}) at 24 °C.

RT microspectrofluorimetry Fluorescence emission spectra were recorded at RT from single living cells using a microspectrofluorimeter (RCS, Firenze, Italy), associated with a Zeiss model Axiophot epifluorescence photomicroscope (Pancaldi et al. 2002). Cells were mounted in TAP medium on polylysine-coated microslides (Menzel-Gläser, Braunschweig, Germany) and at least five independent measurements were performed for each sample analyzed. The exciting light was provided by the light source for epifluorescence of the microscope, an HBO 100 W pressure mercury vapor lamp. The excitation wavelength at 436 nm was obtained with a BP436/10 filter (Zeiss) and was focussed on a single cell at a time using a 1.6 mm diaphragm in combination with a Zeiss Plan-Neofluar 100× objective. The emitted light was collected by the same objective lens and deviated to the detector system, which included a monochromator reticle (band pass 0.25 nm) and a photomultiplier tube. *Autolab* software (RCS, Firenze, Italy) was employed to set the recording range (620–780 nm), optimize the photomultiplier response and visualize the emission spectra. Calibration of the monochromator was verified by recording the spectrum of the excitation light. The linearity of the detector response as a function of incoming fluorescence was analyzed by recording fluorescence spectra from groups formed by 1 to 5 cells of the WT strain under the same conditions of photomultiplication. It was verified that the total emission intensity, calculated by integration as the area subtended under each spectrum (Ferroni et al. 2009), was linearly correlated with the number of cells under the excitation spot (R^2=0.995). Furthermore, increase in intensity as a function of the number of cells analysed did not cause changes in the spectrum profile, as was ascertained after normalization of the spectra to their maximum and calculation of difference spectra.

Elaboration of the spectra was performed with the Origin 6.0 software (OriginLab, Northampton, MA, USA). Fluorescence spectra were corrected for the baseline and routinely smoothed with two cycles of 10-point Fast Fourier Transform filtering procedure, which does not modify the structure of the spectrum. The fourth-order derivative analysis of the spectra was performed to obtain the first information on spectral components, taking into account the limitations of the method (Böddi and Franck 1998). The Gaussian fitting procedure was carried out following already described methods (Šiffel and Braunová 1999; Ferroni et al. 2009).

77 K spectrofluorimetry Fluorescence emission spectra were recorded from cell suspensions at 77 K with an LS50 Perkin-Elmer spectrofluorimeter. Cells suspensions were recorded in TAP medium with 50% glycerol. Excitation was at 435 nm (bandwidth 10 nm) and emission between 600 and 800 nm (bandwidth 3 nm).

Modulated chlorophyll fluorescence Pulse amplitude modulated (PAM) fluorescence was analyzed with an ADC OS1-FL portable fluorometer (ADC Bioscientific Ltd, Hoddesdon, Hertfordshire, UK). Aliquots of cell suspensions were centrifuged at 10,000*g* for 3 min and the pellets were deposited onto pieces of wet filter paper (Schleicher & Schuell). The fluorescence measurements were performed in samples dark-adapted for at least 10 min.

Standard protocols were followed for the calculation of induction/relaxation curves of fluorescence parameters (Niyogi et al. 1997). In particular, for fluorescence quenching analyses, the dark-adapted pellets deposited on wet paper were illuminated for 5 min with an irradiance of either 800 or 1,200 μmol photons m^{-2} s^{-1} provided by an halogen lamp and focussed on the pellets through fiber-optics. A saturation pulse was applied every minute. After the induction phase, for recovery the pellets were maintained in darkness and a saturation pulse was applied after 2 and 5 min. The fluorescence parameters and coefficients used are reported in Roháček (2002) and Baker (2008). For the evaluation of the fraction of "open" PSII (oxidation state of Q_A) the q_L coefficient was calculated according to Kramer et al. (2004). The Stern-Volmer type parameter *NPQ* was used to quantify the non-photochemical quenching. The photoinhibitory component *qI* of *NPQ* was extrapolated as the slowly relaxing component of *NPQ* from the relaxation kinetics (Bailey et al. 2004; Kalituho et al. 2006).

Results and discussion

Three emission bands contribute to the PSII region at RT

The RT fluorescence emission spectra recorded from WT cells showed the typical peak at 683 nm and a broad shoulder at 710–740 nm (Fig. 1a). Franck et al. (2005) reported that in RT spectra the relative contribution of these two components is strongly affected by screening effects due to chlorophyll concentration. The main consequences of this phenomenon are the increase in the contribution of the shoulder at 710–740 nm and a red-shift of the main band. Microspectrofluorimetry allows overcoming this limitation and spectra obtained were very similar to the RT spectra recorded from diluted chloroplast suspensions, i.e. a condition in which re-

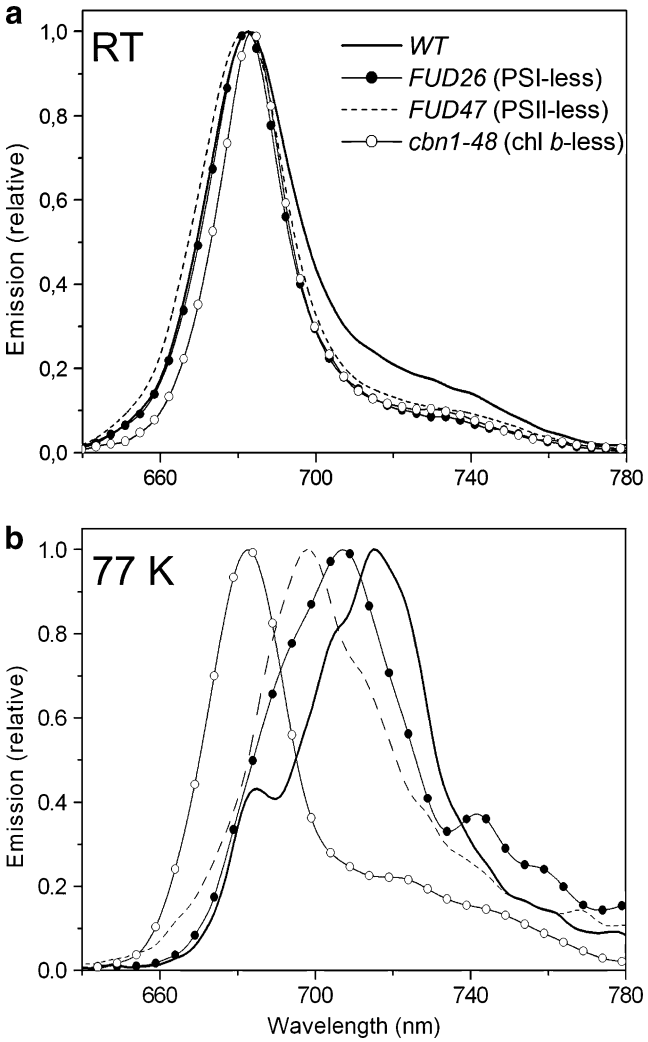

Fig. 1 Fluorescence emission spectra recorded from WT, *FUD26*, *FUD47*, and *cbn1-48 Chlamydomonas reinhardtii* cells at room temperature (RT, **a**) and at 77 K (**b**). **a** RT spectra were recorded from single living cells using a microspectrofluorimeter (excitation, 436 nm). **b** The 77 K spectra were recorded from cell suspensions (excitation, 435 nm). For easier comparison, spectra were each normalized to their maximum peak

absorption of emitted light is negligible (Franck et al. 2002). The 683 nm peak is attributed mainly to PSII, while the long-wavelength emission is assigned to PSI-LHCI with the contribution of vibrational satellites of PSII (Franck et al. 2002, 2005; Ventrella et al. 2007; Lambrev et al. 2010). This assignment finds an evident counterpart in 77 K spectra, in particular the peak at ca. 685 nm is attributed to PSII, while LHCI-PSI dominates emission at long wavelength and in *Chlamydomonas* originates the peak at 715 nm, i.e. blue-shifted with respect to the 720–740 nm emission attributed to the same complex in land plants (Garnier et al. 1986) (Fig. 1b).

In order to confirm that PSII is the main emission source in the 675–695 nm region also at RT, the spectra obtained from WT cells and the mutant *FUD26* were compared. *FUD26* is defective in PSI for a four base pairs deletion in the *psaB* gene, causing a frameshift and truncation of the PsaB polypeptide of PSI core (Girard-Bascou 1987). Although *FUD26* should be incapable of synthesising active PSI units, it has been reported that it can actually revert to even high levels of *psaB* expression (Redding et al. 1999). Therefore, we recorded 77 K spectra from the mutant available in our laboratory. The *FUD26* strain showed a blue-shift of the 715 nm band to 707 nm (Fig. 1b), similar to the *Fl5* PSI-less mutant of *C. reinhardtii* (Garnier et al. 1986). Such shift in emission is indicative of depletion in PSI core in the presence of the whole complement of Lhca antennae (Knoetzel et al. 1998). We also analysed the ability of *FUD26* to re-oxidize the Q_A and thus maintain open PSII thorough the activity of PSI. For an accurate assessment of the redox state of Q_A, the q_L coefficient was used (Kramer et al. 2004). Starting from the dark-adapted state (q_L=1, Q_A fully oxidized), as light was turned on the q_L value declined to ca. 0.5 in WT cells, indicating that the ability of PSI to extract electrons from the chain allowed the maintenance of 50% Q_A in the oxidised state. Conversely, in *FUD26* the value fell down to 0, further confirming the deficiency of PSI (Fig. 2).

We looked for the effect of PSI depletion on the RT fluorescence spectra. After normalization to the maximum, *FUD26* showed an evident loss of long-wavelength emission, especially over 696 nm (ca. −60%) (Fig. 1a).

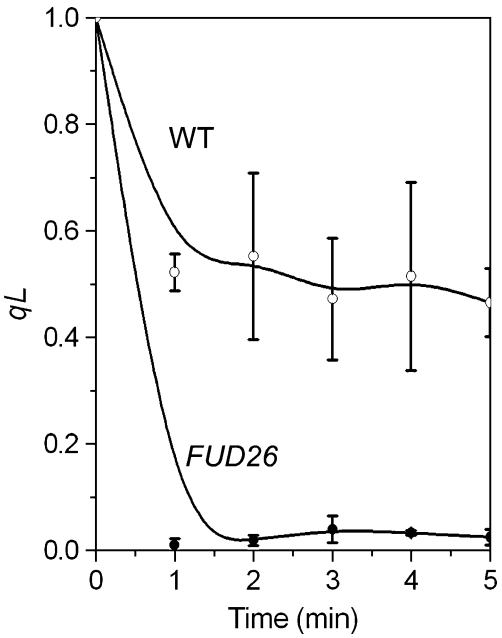

Fig. 2 Fraction of open PSII centers in WT and *FUD26 Chlamydomonas reinhardtii* cells. The fraction of open PSII, i.e. with Q_A oxidized, was evaluated as *qL* during a 5 min-long exposure to 1,200 μmol photons m^{-2} s^{-1}. Values are means with standard deviations (n=3)

This result confirmed the contribution of PSI to the mentioned region and pointed to the correctness of the assumption that PSII generates the main emission peak at 683 nm at RT in vivo (Franck et al. 2002; Ferroni et al. 2009; Lambrev et al. 2010). The residual fluorescence at long wavelength can be assigned to LHCI and to the contribution of PSII satellite vibrational bands (Franck et al. 2002; Ventrella et al. 2007).

In order to dissect the emission sources contributing to the PSII emission region in RT spectra of WT cells, a 4th derivative analysis of these spectra was performed (Fig. 3a). The main positive component was asymmetrical, with a peak at 680 nm and a shoulder at 685 nm, and therefore was hypothesised to arise from two clustering bands. The close proximity of individual bands can indeed generate compound peaks, but also introduce uncertainties in the determination of the actual peak location (Böddi and Franck 1998). In the PSII region, the 4th derivative also indicated the presence of a component at ca. 695 nm. The same three peaks were found in the 4th derivative of the 77 K emission (not shown). In deconvoluted RT and 77 K spectra, the three bands were resolved in the PSII emission region and hereafter referred to as F680, F686 and F694 (Fig. 3a, b). F680 was especially emphasized at RT by comparison with the same band resolved in 77 K spectra. In 77 K spectra, F686 and F694 are usually assigned to the PSII core and F680 is attributed to "free" LHCII. Another band found at both RT and 77 K had a maximum at ca. 702 nm (F702). In the long-wavelength region three main bands were resolved at approx. 713, 720, 735 nm. Although these bands well correspond to the emissions assigned to LHCI-PSI at 77 K (Klimmek et al. 2005; Engelmann et al. 2006), the contribution of the side band(s) of PSII complicates greatly the interpretation of this spectral region at RT (Franck et al. 2002). For this reason, these emissions are no further discussed in this work. At short wavelength, minor bands were found at 670 and 661 nm, not resolved at 77 K, as expected.

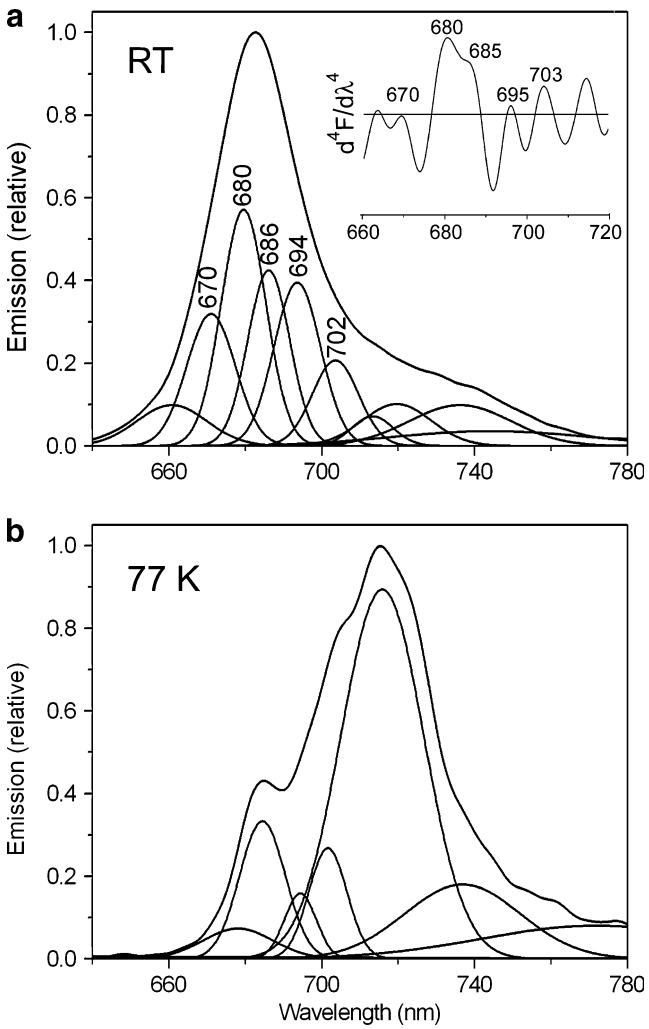

Fig. 3 Analysis of fluorescence emission spectra recorded from WT *Chlamydomonas reinhardtii* cells. **a** Gaussian deconvoluted room-temperature emission spectrum and 4th derivative (insert); the emission wavelengths contributing to the PSII region are indicated. **b** Gaussian deconvoluted 77 K emission spectrum

PSII core and LHCII cooperate in determining the geometry of RT spectra

We examined the possibility of attributing F680, F686 and F694 to specific subcomplexes, in particular PSII core and LHCII. To this aim, we analyzed two mutants depleted either of LHCII or PSII core.

The *cbn1* mutation leads to a lack of chlorophyll *b* (Chunaev et al. 1991); *cbn1-48* has been reported to have a severe reduction in LHCII and also a decline in LHCI, while it retains the minor antennae CP26 and CP29 bound to PSII (Allen and Staehelin 1994). Chlorophyll *b*-less mutants of *C. reinhardtii* and higher plants show 77 K emission spectra altered in peak intensity and position, mostly depending on the amount of Lhca and Lhcb retained in thylakoids (Garnier et al. 1986; Knoetzel et al. 1998; Lin et al. 2003; Ossenbühl et al. 2004). In *cbn1-48*, the very strong decrease in the long-wavelength region at 77 K closely recalled the LHC-depleted *vir-k*[32] mutant of barley and implicated a nearly complete absence of LHCs (Knoetzel et al. 1998) (Fig 1b). A comparison between the normalised RT spectra of *cbn1-48* and WT cells highlighted the fundamental contribution of LHCII to the geometry of the spectrum (Fig. 1a). The kurtosis index, used to assess the deviation from normality (Joanes and Gill 1988), was calculated to compare the peakedness of the spectra: the 2.4 value in *cbn1-48* vs. 0.75 in WT cells quantifies the more "peaked" shape of the spectrum of the mutant. The spectrum broadening caused by LHCII accumulation had been shown in RT spectra of variable

fluorescence of dark-grown barley leaves during the greening process (Franck et al. 2005). It was suggested that the relative loss in emission at short wavelength is due to the decreased contribution of chlorophyll *b* fluorescence in the 640–670 nm region (Franck et al. 2005). In accordance, in *cbn1-48* the minor band at 661 nm resolved in the WT spectrum disappeared, supporting its assignment to chlorophyll *b* (Fig 4). Furthermore, the strong decrease in the amplitude of the 670 nm band suggests that the poorly coupled chlorophylls *a* (and *b*) originating this short-wavelength emission may be mostly located in LHCII (Santabarbara and Jennings 2005). However, even more evident was the depletion in F680, which was not resolved and presumably substituted by a residual emission at 675 nm. This response is strongly indicative of the origin of F680 in the LHCII, in agreement with the emission maximum of free LHCII trimers at RT (Kirchhoff et al. 2003). Noticeably, it was pointed out that the presence of LHCII has only weak influence on the position of the main PSII emission band (Franck et al. 2005). Accordingly, a band at 684 nm accounted for most fluorescence at RT and should be regarded as the main PSII core emission, corresponding to a slightly blue-shifted F686. Interestingly, the second band usually attributed to PSII core, F694, was much reduced in intensity with respect to the WT, as was also the F702 emission (Fig. 5). The residual emission in the long wavelength region is easily attributed to PSI and vibrational satellites of PSII.

The results obtained with *cbn1-48* were indicative of the contribution of LHCs to the emission at RT. To obtain further information, the PSII-core less *FUD47* mutant was analyzed. This strain lacks the D2 protein of the reaction

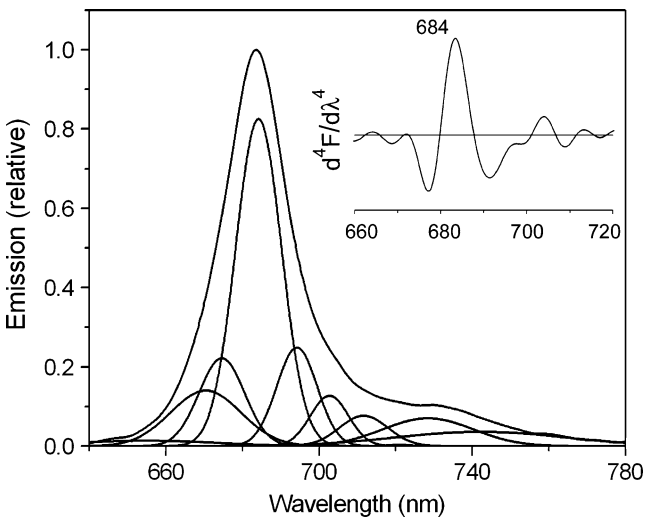

Fig. 4 Gaussian deconvoluted fluorescence emission spectra recorded from LHC-less *cbn1-48 Chlamydomonas reinhardtii* cells at room-temperature. The 4th derivative of the spectrum is reported in the insert

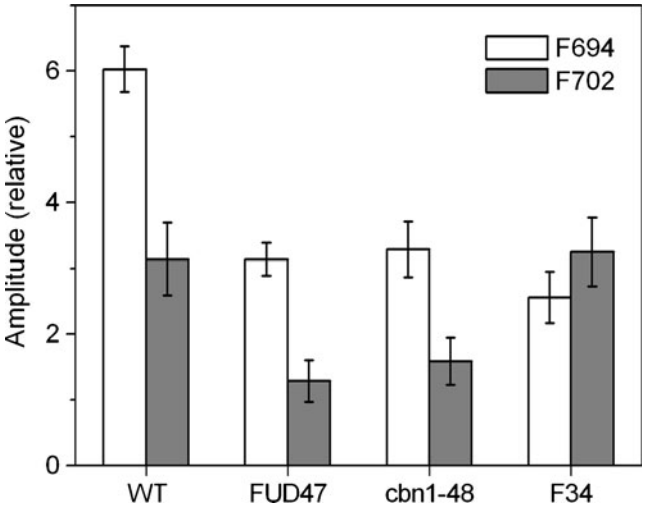

Fig. 5 Relative emission intensity of F694 and F702 in WT and mutant cells of *Chlamydomonas reinhardtii*. The values (means of 5 determinations with SD) have been determined as areas subtended under the corresponding Gaussian curves resolved in spectra normalised to their respective maxima, as reported in Figs. 3a, 4, 6a and 7b

centre and thus is completely defective in the assembly of PSII core (Erickson et al. 1986; de Vitry et al. 1989). In *FUD47*, PSII activity as F_V/F_M was not measurable and the 77 K emission spectra recalled that of the PSII-less *C. reinhardtii* mutant *Fl50* with a single prominent peak at 699 nm (Garnier et al. 1986) (Fig. 1b). Interestingly, the RT spectrum profile was not much altered, i.e. only ca. 2 nm blue-shifted, in *FUD47* with respect to the WT (Fig. 1a). Garnier et al. (1986) already observed that paradoxically RT emission spectra of PSII-less strains were very similar to WT spectra. Nevertheless, the 4th derivative analysis and deconvolution of *FUD47* spectra pointed to interesting changes. The spectrum was dominated by two bands at 677 and 687 nm (Fig. 6a). The comparison with the deconvoluted 77 K spectrum indicated that the band at 677 nm could very likely be assigned to free LHCII, suggesting that in the absence of PSII a blue-shift occurs at RT in the 680 nm emission of this complex (Fig. 6b). The band at 687 nm can be attributed to LHCI-PSI complexes (Croce et al. 1996; Subranyam et al. 2006), although it cannot be excluded a contribution by some small amounts of CP43, whose synthesis is less strictly dependent on the formation of the D1/D2 heterodimer than CP47 (de Vitry et al. 1989; Ma et al. 2007). Interestingly, in spite of the dominant 77 K emission at 699 nm, F694 and F702 were both decreased in amplitude in *FUD47* at RT (Fig. 5).

F34 is another PSII-depleted mutant because of a defect in translation of the *psbC* gene encoding for the CP43 apoprotein (Zerges and Rochaix 1984; de Vitry et al. 1989; Rochaix et al. 1989). We found that the *'F34'* mutant available in our laboratory actually retained a good level of

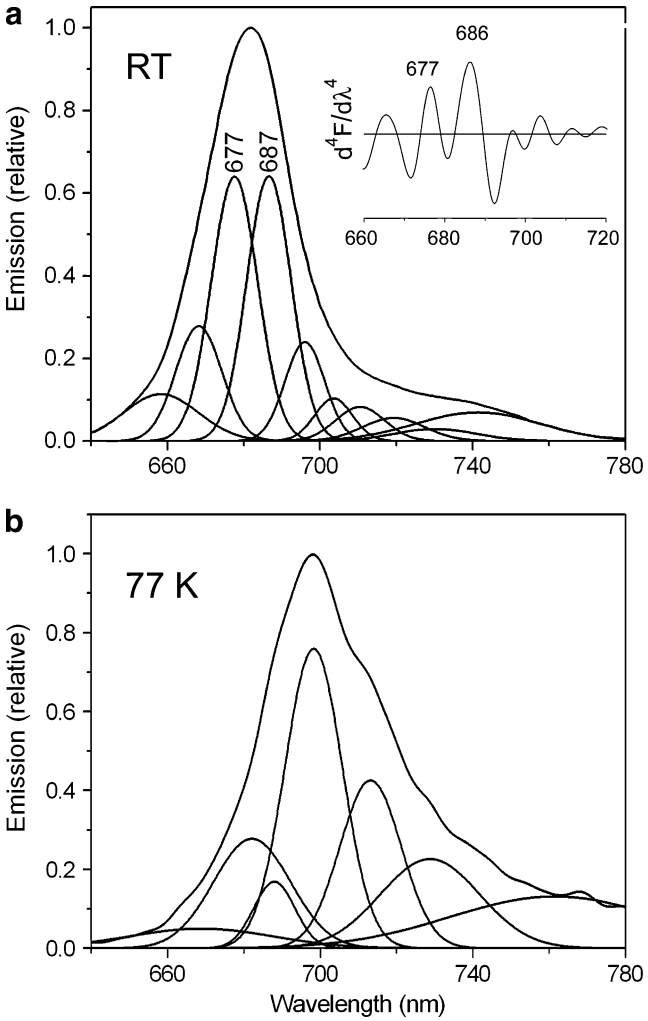

Fig. 6 Analysis of fluorescence emission spectra recorded from PSII-less *FUD47 Chlamydomonas reinhardtii* cells. **a** Gaussian deconvoluted room-temperature emission spectrum and 4th derivative (insert); the emission wavelengths contributing to the PSII region are indicated. **b** Gaussian deconvoluted 77 K emission spectrum

PSII activity, suggesting a certain degree of mutation suppression (Fig. 7a). In this *'F34'*, the main RT band was resolved at 688 nm, which can be accounted by PSII core (Fig. 7b). The F680 was resolved as a relatively minor band, while an intense band was found at 675 nm. Similar to *FUD47* and *cbn1-48*, in *'F34'* the F694 also showed reduced amplitude with respect to the WT (Fig. 5). Interestingly, *'F34'* yielded very high fluorescence at RT (+70% with respect to WT) and was able to only develop very low *NPQ* (Fig. 7c). Since thermal dissipation is considered to be closely dependent on the proper assembly of LHCII-PSII supercomplexes (Horton et al. 2008), we put forward the hypothesis that the amplitude of PSII band F694 may be modulated in vivo by the association of LHCII with PSII. Conversely, in *'F34'* F702 was re-established at the WT level (Fig. 5).

Photoinhibition differentially affects F694 and F702

We hypothesized that not only strong alterations in the thylakoid composition, such as in the mentioned mutants, but also functional rearrangements could be reflected in RT spectra. In fact, in WT cells, the LHCII-PSII assembly is highly flexible to ensure stability of photosynthesis under changing environmental conditions (Horton et al. 2008). A physiological way to disturb LHCII-PSII assembly is to induce PSII photoinhibition with high light.

It was investigated whether and how PSII photoinhibition could affect the amplitude of F680, F686, F694 and F702. Control spectra were recorded at RT from non-photoinhibited WT cells grown under low light. PSII photoinhibition was achieved by a 5-min long irradiation with either 800 or 1,200 μmol photons m^{-2} s^{-1}; some samples were treated with 1,200 μmol photons m^{-2} s^{-1} at the temperature of 4 °C. Photoinhibition was quantified as *qI* by resolving the slowly relaxing component of *NPQ* after 5 min recovery in darkness (Kalituho et al. 2006) (Fig. 8a,b). Immediately after the recovery period, the RT fluorescence spectra were recorded; the amplitudes of F680, F686, F694 and F702 under the four conditions were calculated after spectra normalisation (Fig. 8c). The main band attributed to PSII core, F686, did not show any pattern consistent with photoinhibition treatments. Conversely, the other band usually attributed to PSII core, F694, decreased linearly with *qI* (linear regression R^2=0.924, P<0.05), suggesting a direct implication of this emission in photoinhibition (Fig. 9). Although F680 yielded in each photoinhibited condition higher amplitude than in the control, increase was not significant. Finally, amplitude of F702 increased in samples photoinhibited at RT, but it was quenched at 4 °C to the level found in WT cells.

Assignment of fluorescence emission bands and revision of fluorescence emission ratios

Based on the results obtained with WT and mutant *Chlamydomonas reinhardtii*, we propose the following fluorescence bands assignments at RT.

F680 disappears in the absence of LHCII, supporting its assignment to free LHCII (Kirchhoff et al. 2003). Its emission wavelength is found between 677 nm (PSII-less *FUD47*) and 680 nm (WT). This can be indicative of a role of the PSII core in determining the position of the free LHCII peak. Photoinhibition of WT cells causes only negligible increase in the amplitude of F680 at RT (Fig. 8c).

F686 is proposed to be the fundamental emission of the PSII core. In spite of the previous assignment to CP43 (Pancaldi et al. 2002), presently we prefer to avoid any attribution of F686 to PSII subcomplexes (see also van Dorssen et al. 1987; Krausz et al. 2005; Ferroni et al. 2009).

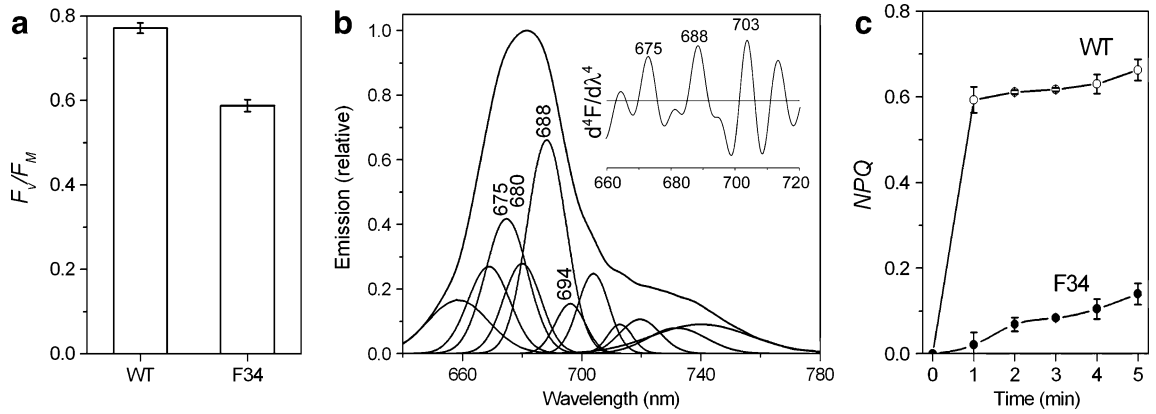

Fig. 7 Fluorescence emission analysis of *'F34' Chlamydomonas reinhardtii* cells. **a** Maximum quantum efficiency of PSII photochemistry (means of 5 determinations with SD). **b** Gaussian deconvoluted room-temperature emission spectrum and 4th derivative (insert); the emission wavelengths contributing to the PSII region are indicated. **c** Induction kinetics of non-photochemical quenching of chlorophyll fluorescence (*NPQ*) during a 5 min-long exposure of dark-adapted cells to 1,200 μmol photons m^{-2} s^{-1} (values are means of 3 determinations with SD)

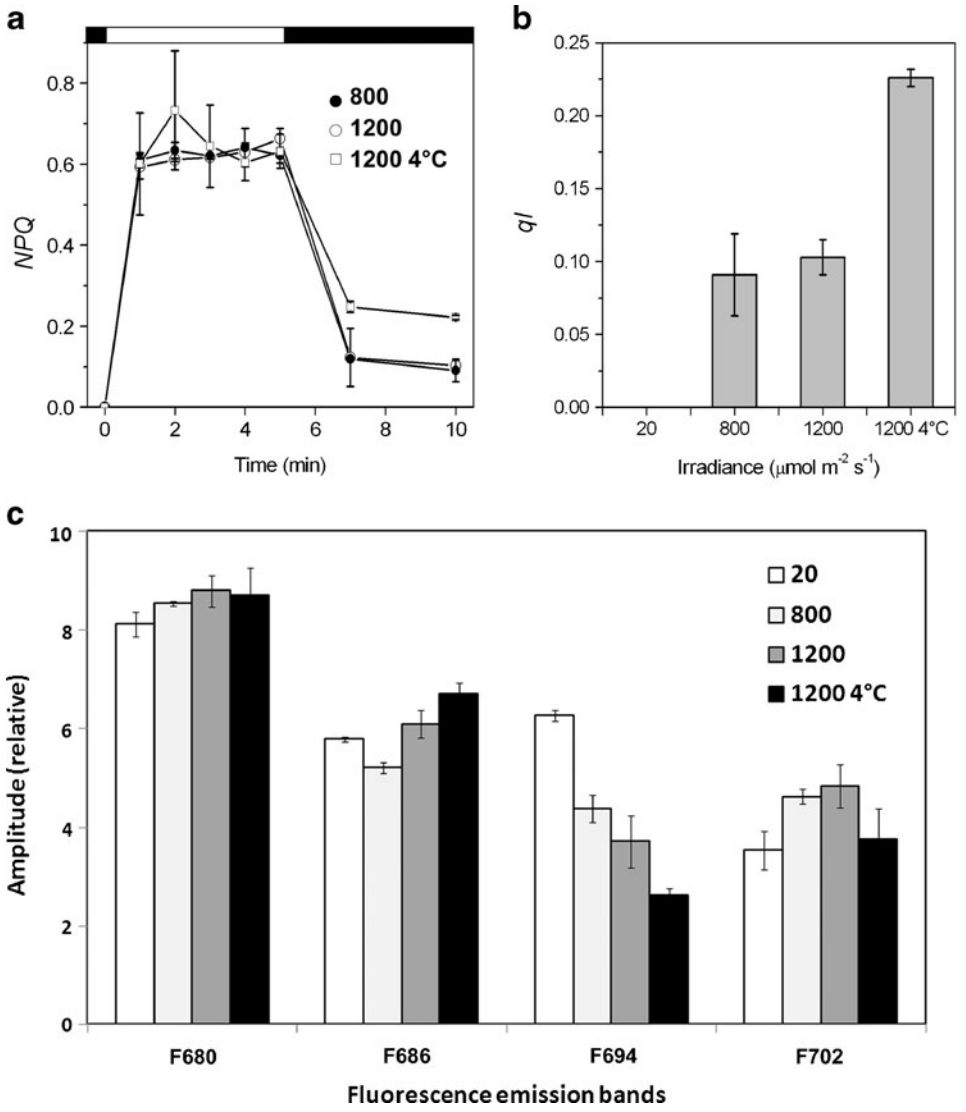

Fig. 8 Photoinhibition experiments with WT *Chlamydomonas reinhardtii* cells. **a** Induction and relaxation kinetics of *NPQ* under three different conditions, as indicated in the figure. **b** Quantification of *qI*, the photoinhibitory component of *NPQ*. **c** Relative emission intensity of F680, F686, F694 and F702 after the relaxation phase in high-light treated cells; irradiance values reported in the figure legend are expressed as μmol photons m^{-2} s^{-1}; amplitude values have been determined as areas subtended under the corresponding Gaussian curves resolved in spectra normalized to their respective maxima (not shown). In each case, all values are means of 3 replicates with SD

In all samples analyzed, F694 was detected at least at a basal level. Reduction in F694 in PSII-less and LHCII-less mutants shows that both PSII and LHCII cooperate in determining the final amplitude of this band. In particular, contribution of PSII core to F694 is here considered valid (Pancaldi et al. 2002), but *cbn1-48* shows that PSII core alone is not able to emit an F694 at the WT level in the absence of LHCII. We propose that the intensity of F694 increases as a consequence of the association of LHCII with PSII core. All conditions impairing the LHCII-PSII assembly, either lack of components or photoinhibition, will cause a decrease in F694 down to the basal level (Figs. 5, and 8c).

Finally, F702 is most probably due to the contribution of at least two main complexes, i.e. LHCII aggregates and LHCI-PSI, which complicates the interpretation of this band. We suggest that under moderately photoinhibited states the released LHCII feeds the aggregated LHCII subpopulation leading to a significant increase in F702. However, under stronger photoinhibition (or even absence of PSII cores, as in *FUD47*) F702 reduces its amplitude (Fig. 8c). Although it was not analyzed in this work, inhibition of PSI may also account for such reduction at least in part (Alboresi et al. 2009).

The data obtained with the photoinhibition experiments have been used to calculated two fluorescence emission ratios. The fluorescence ratio F680/(F686+F694) markedly increased with *qI* (Fig. 10a). This ratio was previously used to obtain indications on the assembly state of PSII core in a variety of organisms (Pancaldi et al. 2002; Ferroni et al. 2007a, 2007b; Baldisserotto et al. 2005, 2010). F680 was indeed attributed to PSII reaction centre, F686 and F694 to the inner antennae CP43 and CP47, respectively, and the variations in the ratio were discussed in terms of defective assembly of PSII core units (Pancaldi et al. 2002). Here we show that increase in the ratio just points to a defect in PSII, but seems rather to be the consequence of the LHCII-PSII uncoupling, which reduces the amplitude of F694. The simultaneous variation in F694 and F686 leads to the plateau level found in the ratio at high *qI*, so that the ratio hardly distinguishes between different degrees of photoinhibition (Fig. 10a). An alternative ratio could be proposed, i.e. F680/F694, which increases linearly with *qI* (Fig. 10a).

The F702/(F686+F694) ratio was used as an index of the assembly state of LHCII with PSII, because in the original assignment F702 was interpreted as LHCII disconnected from PSII core (Pancaldi et al. 2002; Ferroni et al. 2009). In the light of the present results, the contribution of aggregated LHCII to F702 is considered valid, though not exclusive, because of the concomitant emission from LHCI-PSI. The ratio represents a normalisation of F702 to the bulk emission of PSII and closely reflects the trend of

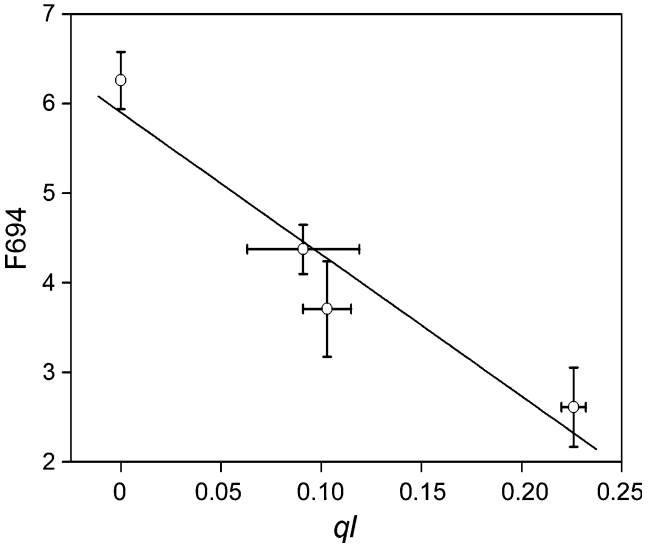

Fig. 9 Correlation between F694 and *qI*. The values were obtained in WT *Chlamydomonas reinhardtii* cells during the photoinhibition experiments described in Fig. 8 (means of 3 replicates with SD)

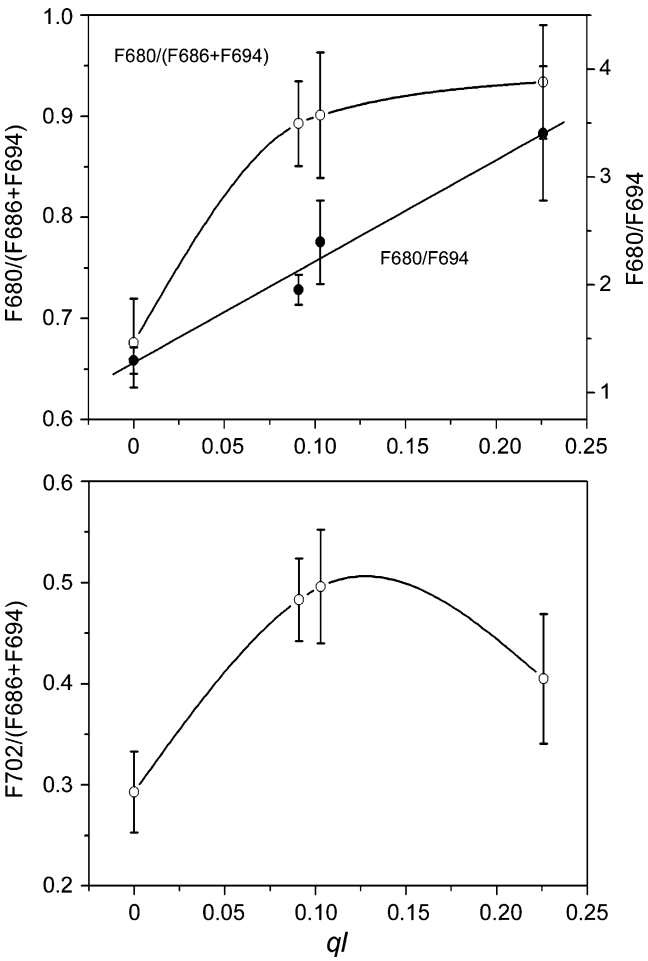

Fig. 10 Relationship between fluorescence emission ratios and *qI*. The ratios were calculated using the amplitudes obtained during the photoinhibition experiments as reported in Fig. 8 (means of 3 replicates with SD)

F702 (Fig. 10b). It appears that LHCII aggregation can be highlighted by the ratio only under moderate *qI*, while it could be overlooked at high *qI*, which implicates a limitation in the use of this parameter in *C. reinhardtii*.

Conclusions

Since the speculative nature of current assignments of RT bands undoubtedly limits the power of techniques such as microspectrofluorimetry, we have analyzed RT emission spectra from mutants and WT cells of *C. reinhardtii*.

It emerges that not only LHCII is a main actor in determining RT emission profiles in vivo, but the well-known dynamism in LHCII assembly is sufficient to explain the variations in amplitudes of F680, F694 and F702. We propose that free LHCII originates F680, LHCII-PSII association increases the amplitude of F694 and LHCII aggregation affects the amplitude of F702. The F686 band is assigned to PSII core. These new attributions partly rectify those previously proposed (Pancaldi et al. 2002; Ferroni et al. 2009); in particular, attribution of F680 to the RC of PSII, which has been documented in non-green algae (Pancaldi et al. 2002; Baldisserotto et al. 2005), is not valid in *C. reinhardtii*.

Based on the new assignments, we have also revisited the meaning of two fluorescence emission ratios. F680/(F686+F694) mainly reflects the assembly of LHCII-PSII and can be used as a sensitive parameter under moderately photoinhibited states. Its use can be especially advantageous for analysis of samples where F686 and F694 cannot be resolved as independent emissions (Ferroni et al. 2007b). However, where these emissions are well resolved, the use of the alternative F680/F694 ratio can be more informative. F702/(F686+F694) allows to highlight the occurrence of aggregated LHCII under moderate photoinhibitory conditions, but it can fail to reveal it under more severe photoinhibition. Therefore, the two ratios are useful tools for the characterisation of the LHCII association state under not exceedingly severe stress conditions. Conversely, in the most photoinhibited samples, F694 decreases to the basal level and, concomitantly, F702 nearly re-establishes to the control level, making these spectra somewhat similar to those recorded from *'F34'* mutant. Therefore, we conclude that outside of the mentioned application limits of fluorescence ratios, the RT spectra tend to degenerate showing characteristics of mutants that are partly depleted in PSII.

Acknowledgements This work was financially supported by the Italian Ministry for University and Research (MIUR) under the project PRIN2007 "Protein turn-over and accumulation in plants" (20073YHRLE) and by the University of Ferrara.

References

Alboresi A, Ballottari M, Hienerwadel R, Giacometti GM, Morosinotto T (2009) BMC Plant Biol 9:71
Alfonso M, Montoya G, Cases R, Rodriguez R, Picorel R (1994) Biochem 33:10494–10500
Allen KD, Staehelin LA (1994) Planta 194:42–54
Andersson J, Walters RG, Horton P, Jansson S (2001) Plant Cell 13:1193–1204
Andrizhiyevskaya EG, Chojnicka A, Bautista JA, Diner BA, van Grondelle R, Dekker JP (2005) Photosynth Res 84:173–180
Bailey S, Horton P, Walters RG (2004) Planta 218:793–802
Baker NR (2008) Annu Rev Plant Biol 59:89–113
Baldisserotto C, Ferroni L, Medici V, Pagnoni A, Pellizzari M, Fasulo MP, Fagioli F, Bonora A, Pancaldi S (2004) Plant Biol 6:578–589
Baldisserotto C, Ferroni L, Moro I, Fasulo MP, Pancaldi S (2005) Protoplasma 226:125–135
Baldisserotto C, Ferroni L, Zanzi C, Marchesini R, Pagnoni A, Pancaldi S (2010) Protoplasma 240:83–97
Barber J (2002) Curr Opin Struct Biol 12:523–530
Ben-Shem A, Frolow F, Nelson N (2003) Nature 426:630–635
Boardman NK, Thorne SW, Anderson JM (1966) Biochem 56:586–593
Böddi B, Franck F (1998) J Photochem Photobiol B Biol 41:73–82
Bricker TM, Frankel LK (2002) Photosynth Res 72:131–146
Chunaev AS, Mirnaya ON, Maslov VG, Boschetti A (1991) Photosynthetica 25:291–301
Croce R, Zucchelli G, Garlaschi FM, Bassi R, Jennings RC (1996) Biochem 35:8572–8579
de Bianchi S, Dall'Osto L, Tognon G, Morosinotto T, Bassi R (2008) Plant Cell 20:1012–1028
de Vitry C, Olive J, Drapier D, Recouvreur M, Wollman FA (1989) J Cell Biol 109:991–1006
Engelmann E, Zucchelli G, Casazza AP, Brogioli D, Garlaschi FM, Jennings RC (2006) Biochem 45:6947–6955
Erickson JM, Rahire M, Malnoe P, Girard-Bascou J, Pierre Y, Bennoun P, Rochaix J-D (1986) EMBO J 5:1745–1754
Ferroni L, Baldisserotto C, Pantaleoni L, Billi P, Fasulo MP, Pancaldi S (2007a) Am J Bot 94:1972–1983
Ferroni L, Baldisserotto C, Zennaro V, Soldani C, Fasulo MP, Pancaldi S (2007b) Eur J Phycol 42:91–104
Ferroni L, Baldisserotto C, Pantaleoni L, Fasulo MP, Fagioli P, Pancaldi S (2009) Plant Biol 11:631–641
Franck F, Juneau P, Popovic R (2002) Biochim Biophys Acta 1556:239–246
Franck F, Dewez D, Popovic R (2005) Photochem Photobiol 81:431–436
Garnier J, Maroc J, Guyon D (1986) Biochim Biophys Acta 85:395–406
Girard-Bascou J (1987) Curr Genetics 12:483–488
Groot ML, Frese RN, de Weerd FL, Bromek K, Pettersson A, Peterman EJG, van Stokkum IHM, van Grondelle R, Dekker JP (1999) Biophys J 77:3328–3340
Hemelrjik PW, Kwa SLS, van Grondelle R, Dekker JP (1992) Biochim Biophys Acta 1098:159–166
Horton P, Johnson MP, Perez-Bueno ML, Kiss AZ, Ruban AV (2008) FEBS J 275:1069–1079
Joanes JL, Gill CA (1988) J R Stat Soc D Statistician 47:183–189
Kalituho L, Graßes T, Graf M, Rech J, Jahns P (2006) Planta 223:532–541
Kirchhoff H, Hinz HJ, Rösgen J (2003) Biochim Biophys Acta Bioenerg 1606:105–116
Klimmek F, Ganeteg U, Ihalainen JA, van Roon H, Jensen PE, Scheller HV, Dekker JP, Jansson S (2005) Biochem 44:3065–3073

Knoetzel J, Bossmann B, Grimme LH (1998) FEBS Lett 436:339–342
Kramer DM, Johnson G, Kiirats O, Edwards GE (2004) Photosynth Res 79:209–218
Krausz E, Hughes JL, Smith PJ, Pace RJ, Peterson Årsköld S (2005) Photosynth Res 84:193–199
Lambrev PH, Nilkens M, Miloslavina Y, Jahns J, Holzwarth AR (2010) Plant Physiol 152:1611–1624
Lin Z-F, Peng C-L, Lin G-Z, Zhang J-L (2003) Photosynthetica 41:589–595
Ma J, Peng L, Guo J, Lu Q, Lu C, Zhang L (2007) Plant Cell 19:1980–1993
Niyogi KK, Björkman O, Grossman AR (1997) Plant Cell 9:1369–1380
Ossenbühl F, Göhre V, Meurer J, Krieger-Liszkay A, Rochaix J-D, Eichacker LA (2004) Plant Cell 16:1790–1800
Pancaldi S, Baldisserotto C, Ferroni L, Bonora A, Fasulo MP (2002) J Exp Bot 53:1753–1763
Pantaleoni L, Ferroni L, Baldisserotto C, Aro E-M, Pancaldi S (2009) Planta 230:1019–1031
Redding K, Cournac L, Vassiliev IR, Golbeck JH, Peltier G, Rochaix J-D (1999) J Biol Chem 274:10466–10473
Rochaix JD, Kuchka M, Mayfield S, Schirmerrahire M, Girard-Bascou J, Bennoun P (1989) EMBO J 8:1013–1021
Roháček K (2002) Photosynthetica 40:13–29
Santabarbara S, Jennings RC (2005) Biochim Biophys Acta Bioenerg 1709:138–149
Schmid VHR (2008) Cell Mol Life Sci 65:3619–3639
Šiffel P, Braunová Z (1999) Photosynth Res 61:217–226
Subranyam R, Jolley C, Brune DC, Fromme P, Webber AN (2006) FEBS Lett 580:233–238
van der Weij-de Wit CD, Ihalainen JA, van Grondelle R, Dekker JP (2007) Photosynth Res 93:173–182
van Dorssen RJ, Breton J, Plijter JJ, Satoh K, van Gorkom HJ, Amesz J (1987) Biochim Biophys Acta 893:267–274
Ventrella A, Catucci L, Villari V, Monsù Scolaro L, Agostiniano A (2007) Bioelectrochem 70:33–38
Zerges W, Rochaix J-D (1984) Mol Cell Biol 14:5268–5277